Pergamon

Int. J. Heat Mass Transfer. Vol. 39, No. 10, pp. 2023–2037, 1996

0017-9310/96 $15.00 + 0.00

0017-9310(95)00304-5

Experimental and statistical investigation of changes in surface roughness associated with spray quenching

J. D. BERNARDIN and I. MUDAWAR†

Boiling and Two-phase Flow Laboratory, School of Mechanical Engineering, Purdue University, West Lafayette, IN 47907, U.S.A.

(*Received* 10 *March* 1995 *and in final form* 31 *July* 1995)

Abstract—Surface contact profilometry data measured on aluminum surfaces were statistically analyzed to investigate the changes in surface roughness which occur during heat treatment. The tested samples included commercially pure aluminum (Al-1100) with polished, particle blasted, and milled finishes; and aluminum alloy Al-2024 with polished, particle blasted and extruded finishes. Statistical results along with scanning electron microscope photographs indicate each heat–quench cycle was accompanied by measurable changes in surface roughness, whose magnitude was dependent upon initial surface finish and alloy composition. The changes included both small scale roughness features, which influence cooling rate by increasing the number of bubble nucleation sites during transition and nucleate boiling, and, more importantly, large features which influence the impact and spreading of spray drops as well as the Leidenfrost temperature for spray quenching. The primary cause for roughness was determined to be a hydrogen diffusion phenomenon resulting from breakdown of water vapor at high temperatures inside moisture laden furnaces. Copyright © 1996 Elsevier Science Ltd.

1. INTRODUCTION

Heat treatment and quenching of metallic alloys

Aluminum is the metal of choice in virtually all aerospace structures because of its high strength-to-weight ratio and corrosion resistance. It is also rapidly becoming a viable substitute to steel in the automobile industry in the so-called *aluminum intensive vehicles*. Already in production in Europe and under final development in North America, these vehicles possess frames, body panels and engine blocks which are all made of aluminum. Unlike steel cars which produce much scrap, aluminum vehicles are fully recyclable and their light weight might one day make possible the deployment of the relatively low power electric vehicles.

However, it is widely acknowledged throughout the automotive industry that successful and profitable entry of aluminum vehicles into the market is contingent upon the ability to greatly reduce production cost and develop accurate and efficient process models for the making of high strength aluminum alloy parts. Heat treatment represents a key process for which such models are currently sought; the findings of the present study concern this process in particular.

Heat treatment is a heating and cooling process designed to alter metallurgical microstructure in order to obtain desired mechanical properties. One such process, *solution heat treatment*, is commonly used in the aluminum industry to increase the strength and hardness for a variety of alloys. This process is accomplished in three steps:

(1) solution treatment—heating the part to a temperature near, but slightly below, the melting point of the alloy in order to completely dissolve the alloy solute into the primary metal matrix,

(2) quenching—rapidly cooling the part to the quenchant's temperature in order to freeze the solid microstructure resulting from the heating process, and

(3) aging—reheating the part to some intermediate temperature for a prescribed period of time, allowing the hardening precipitates to coalesce into sites which are finely dispersed within the grains of the primary metal.

Proper solution heat treatment results in a fine dispersion of solute precipitants which act as dislocation barriers, resisting deformations resulting from externally applied stresses. An improper solution heat treatment process consisting of either slow quenching or overaging, results in massive precipitation of the alloy constituents along grain boundaries, producing an alloy with poor strength and poor hardness.

An ideal quench is one that proceeds at an infinitely fast rate since this would preclude any massive coalescence of hardening solutes along grain boundaries. In most practical situations, however, quench rate is slowed by the poor heat transfer effectiveness of the film boiling regime at the onset of the quench. Other factors contributing to a slower quench rate are the large thermal mass of many commercial parts and the

† Author to whom correspondence should be addressed.

NOMENCLATURE

$A(k)$	dimensionless autocovariance function	$p(z)$	surface height distribution
$C(k)$	covariance function	R_a	arithmetic average surface roughness
i	imaginary number, $\sqrt{-1}$	Sk	skewness
$I(\omega)$	Periodogram	x	spatial coordinate along the surface
k	integer corresponding to lag length	z	surface height measurement
Ku	normalized kurtosis	$\bar{z}$	mean surface height.
L	scan length		
l	lag length	Greek symbols	
l_0	distance between consecutive scan points (1 μm)	λ	wavelength
		σ	standard deviation
N	number of data points in a profile scan	ω	spatial frequency.

need to prevent large temperature gradients in parts having cross-sections with large thickness variations. Figure 1a shows, for bath cooling (pool boiling), the boiling regimes associated with quenching a small alloy sample. As illustrated, the rate of quenching is slowest during the film boiling regime and undergoes a rapid increase at the Leidenfrost (minimum heat flux) temperature. Unfortunately, it is at temperatures associated with the film boiling regime that much of the detrimental coalescence of solutes occurs along the grain boundaries. To most heat treatment operations, earlier exit from the film boiling regime (i.e. a higher Leidenfrost temperature) is key to attaining a proper alloy microstructure; hence the practice of using additives which facilitate the breakup of the vapor blanket at higher surface temperatures.

A more popular alternative to bath cooling in many heat treating operations is quenching via water sprays. High velocity droplet impact greatly increases cooling effectiveness in all boiling regimes; thus contributing to a faster rate of quenching and superior microstructure. Additionally, parts with cross-sections having large thickness variations can be cooled by an array of individually configured sprays, producing the desired fast quench rate *uniformly* throughout the cross-section by impacting thicker sections with denser sprays and thinner sections with lighter ones.

Effects of surface roughness in boiling

Surface roughness plays a very important role in the transport of heat from metallic surfaces during boiling. The dependence of the boiling mechanisms on microsurface geometry, while greatly complicating efforts to predict or correlate boiling heat transfer data, has made possible the development of many methods for enhanced heat removal. Since the 1930s, many researchers have capitalized on the sensitivity of nucleate boiling to microsurface geometry, recommending means to alter the surface in order to reduce the superheat required to activate a given cavity, increase boiling site density and/or increase surface area. Interestingly, the earliest known boiling enhancement studies by Jacob and Fritz and by Sauer (see ref. [1]) also pointed to rapid deterioration of the boiling enhancement with time, due to changes in both surface roughness and surface chemistry.

Not all boiling regimes are equally impacted by surface roughness. Direct access of the liquid to the surface during nucleate boiling renders this boiling regime most sensitive to microsurface geometry. Liquid access is much more limited during the transition boiling regime due to an intermittent vapor blanket between the liquid and the surface, rendering any surface roughness features which are smaller than the thickness of the vapor film ineffective at promoting nucleation. This blanket becomes fairly continuous during film boiling where the effect of surface roughness is less clearly realized.

During spray cooling, the part traverses regimes similar to those of bath quenching as evidenced by the similarity of the *shape* of the cooling curve for spray quenching (Fig. 1a) to that for bath quenching. While microsurface geometry is expected to influence boiling in sprays, its effect is far more difficult to ascertain than in bath quenching. Sprays can be classified as either *light*, whose liquid is completely consumed by boiling and vaporization, or *dense*, whose excess liquid is accumulated upon the surface during the quench. Small scale features of about 1–25 μm influence the nucleation of bubbles within the liquid film deposited by each droplet of a light spray, or the liquid layer formed by multiple droplet impact in a dense spray. Large surface features of about 25–1000 μm, on the other hand, produce an effect not commonly encountered in bath quenching, that of greatly altering the spreading of liquid droplets upon impact, especially for the light sprays commonly employed in heat treatment.

Changes in surface roughness associated with heat treatment

The present study was spurred by changes observed by the authors in the cooling curve of aluminum samples following repeated heat–quench cycles [2, 3].

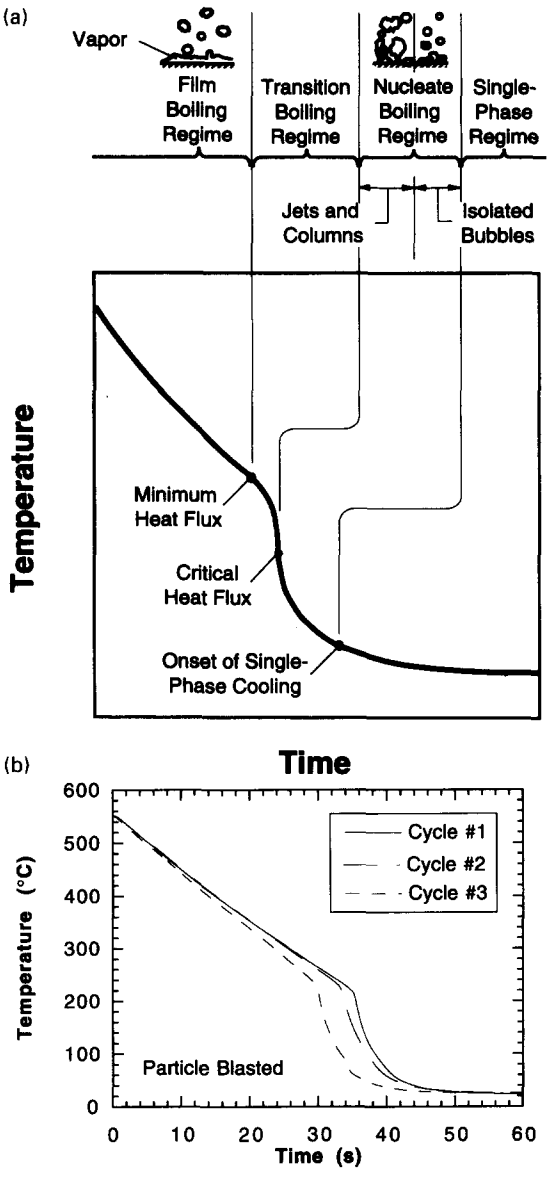

Fig. 1. (a) Boiling regimes associated with bath quenching a small metallic mass, and (b) cooling curve shifts for an Al-1100 sample with a particle blasted surface during repeated heat-spray quench cycles.

Each cycle consisted of preheating aluminum samples followed by quenching to room temperature. Inspection of the surface before and after each heat–quench cycle revealed significant changes in surface roughness which were dependent on initial surface finish. Upon repeating the cycle, it was observed that the cooling curve of the sample experienced a shift toward a shorter quench period, due primarily to an increase in the Leidenfrost temperature, as shown in Fig. 1b. It was speculated that the changes in the cooling curve were the result of surface roughening which occurred during the heat–quench cycle.

There have been many studies in the heat transfer literature concerning the importance of microstructure geometry to boiling. What has been lacking, so far, are (a) an understanding of the *causes* for changes in surface roughness, especially at the high temperatures encountered in materials processing, and (b) systematic methods for quantifying the *magnitude of the roughness changes*.

In this study, a statistical analysis, using surface contact profilometry data, will be used to explore, quantitatively, the effects of a heat–quench cycle on the surface condition for aluminum samples. This study will also explore possible causes for the surface roughening including (1) initial surface roughness, (2) mineral deposition associated with droplet evaporation, (3) oxidation and surface chemical reactions, (4) dynamic forces associated with droplet impact, and (5) heat treatment temperature; and ascertain which of these are the dominant causes for the roughening.

2. EXPERIMENTAL METHODS

Test specimens

The test samples used in this study were fabricated from Al-1100, a 99.0% pure aluminum which is non-heat treatable but used as reference for other commercial alloys, and Al-2024, a copper-based aluminum alloy popular in the aerospace industry. The sample geometries, Fig. 2a, b, were dictated by availability of commercial stock. Each sample was instru-

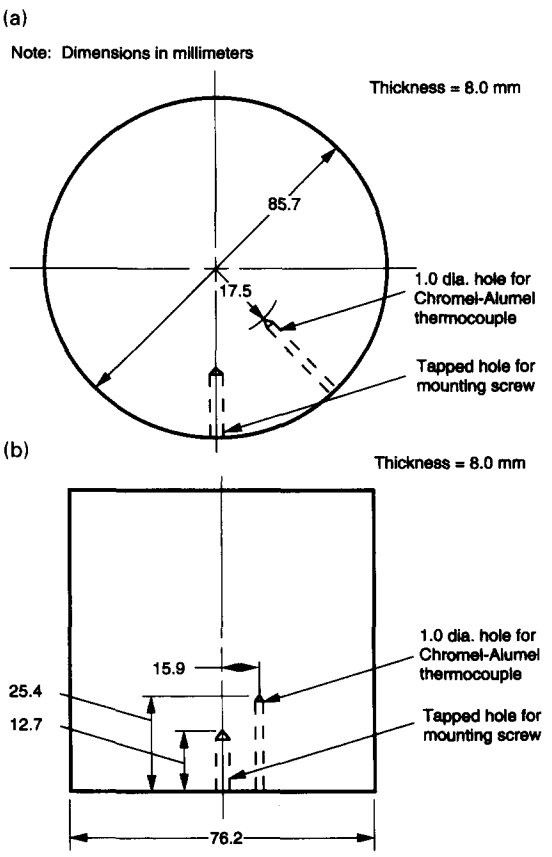

Fig. 2. Schematics of the (a) disk and (b) square test samples.

mented with a single Chromel–Alumel (type K) thermocouple protected in an Inconel sheath.

The surface finish on commercial alloy parts varies widely depending on composition, die tolerances, heat treatment schedule, etc. Therefore, it was deemed prudent to test surfaces having finishes which are both vastly different and reproducible. Three types of surface finishes were applied to the Al-1100 samples: mirror polished, particle blasted, and milled. The Al-2024 samples were prepared with polished and particle blasted surface finishes only since a prior investigation by the authors [3] with Al-1100 samples revealed milled surfaces did not produce significant cooling curve changes following repeated heat–quench cycles. In addition, extruded specimens of Al-2024 were tested to investigate the effects of a heat–quench cycle for an industrial type surface finish.

Test procedure

Prior to the heat–quench cycle, the surface roughness of each sample was measured using an Alpha-Step 1000 profilometer manufactured by Tencor Instruments. A 1.5 μm radius diamond tip stylus with a force of 3 mg traversed the sample surface over a scan length of 2000 μm with a resolution of 1 μm (i.e. 2001 data points per scan). A total of 10 scans were made along symmetrical axes on the surface of each sample, five scans from left to right and five from top to bottom, at a separation distance of approximately 10 mm. A detailed discussion of the finite resolution of the profilometer measurements can be found elsewhere [4].

The heat–quench cycles were performed in a large scale materials processing test bed illustrated in Fig. 3. The test bed is comprised of several components (many of which are not shown in the figure), the most important of which are a high temperature furnace, a sample translation platform, and a spray chamber. The test sample was first mounted on the translation platform and its thermocouple leads were connected to a computer-controlled Keithley series 500 data acquisition system. The heat–quench cycle commenced by raising the test sample into the preheated furnace. After reaching a temperature of 555°C for the Al-1100 samples (or 495°C for the Al-2024 samples), the translation platform was quickly lowered into the spray chamber where one surface of the sample was normally impacted by the spray. The spray possessed a flat impact pattern with a long axis spray angle of 51°, a fluid temperature of 23°C, a nozzle gage pressure of 550 kPa, a liquid flow rate of 18×10^{-6} m^3 s^{-1}, a Sauter mean diameter of 0.286 mm, a mean drop velocity of 13.5 m s^{-1}, and a mean surface spray flux of 5.32×10^{-3} m^3 s^{-1} m^{-2}. Sample temperatures were recorded every 20 ms starting the instant of removal from the furnace; the thermocouple response time was estimated to be about 2 ms. A similar procedure was employed with the air cooled tests except that the samples were allowed to cool by natural convection in open air instead of being spray quenched.

Upon completing the heat–quench cycle, the surface roughness was again measured using the profilometer. Following the surface roughness measurements, a Jeol JSM-T300 scanning electron microscope equipped with an X-ray surface chemical analyzer was used to capture images of microsurface geometry for some of the samples.

3. ROUGHNESS STATISTICAL PARAMETERS

Several statistical parameters were employed in analyzing the surface roughness data. These parameters are only briefly described below. Additional details concerning these and other parameters can be found elsewhere [5, 6].

Mean surface height

The profilometer used in the present study possessed an auto-leveling feature which forces the first and last data points in the scan to assume surface height values equal to zero. Heights of the other scan points, z_i, are referenced with respect to this zero level. A mean surface level, $\bar{z}$, is then measured such that

$$\sum_{i=1}^{N} (z_i - \bar{z}) + 0. \tag{1}$$

where N is the number of data points in the scan.

Arithmetic average roughness and standard deviation

The arithmetic average surface roughness, R_a, is the average of absolute values of deviations in surface height from the mean level.

$$R_a = \frac{1}{N} \sum_{i=1}^{N} |z_i - \bar{z}|. \tag{2}$$

This important parameter is both a simple and powerful tool for comparing roughnesses of different surfaces.

The standard deviation, σ, is another measure of surface height data spread about the mean height and defined as

$$\sigma = \sqrt{\frac{1}{N} \sum_{i=1}^{N} (z_i - \bar{z})^2}. \tag{3}$$

Surface height distribution, skewness and normalized kurtosis

The surface height distribution $p(z)$, is a histogram of the fraction of total data points that lie within an incremental height range. This distribution gives a pictorial representation of the data spread about the mean surface height. Large variations in surface roughness for a given sample would be evident in this histogram.

Skewness is a measure of symmetry of the surface height distribution about its mean value. Mathematically, skewness, Sk, is defined as the third moment of surface height about the mean:

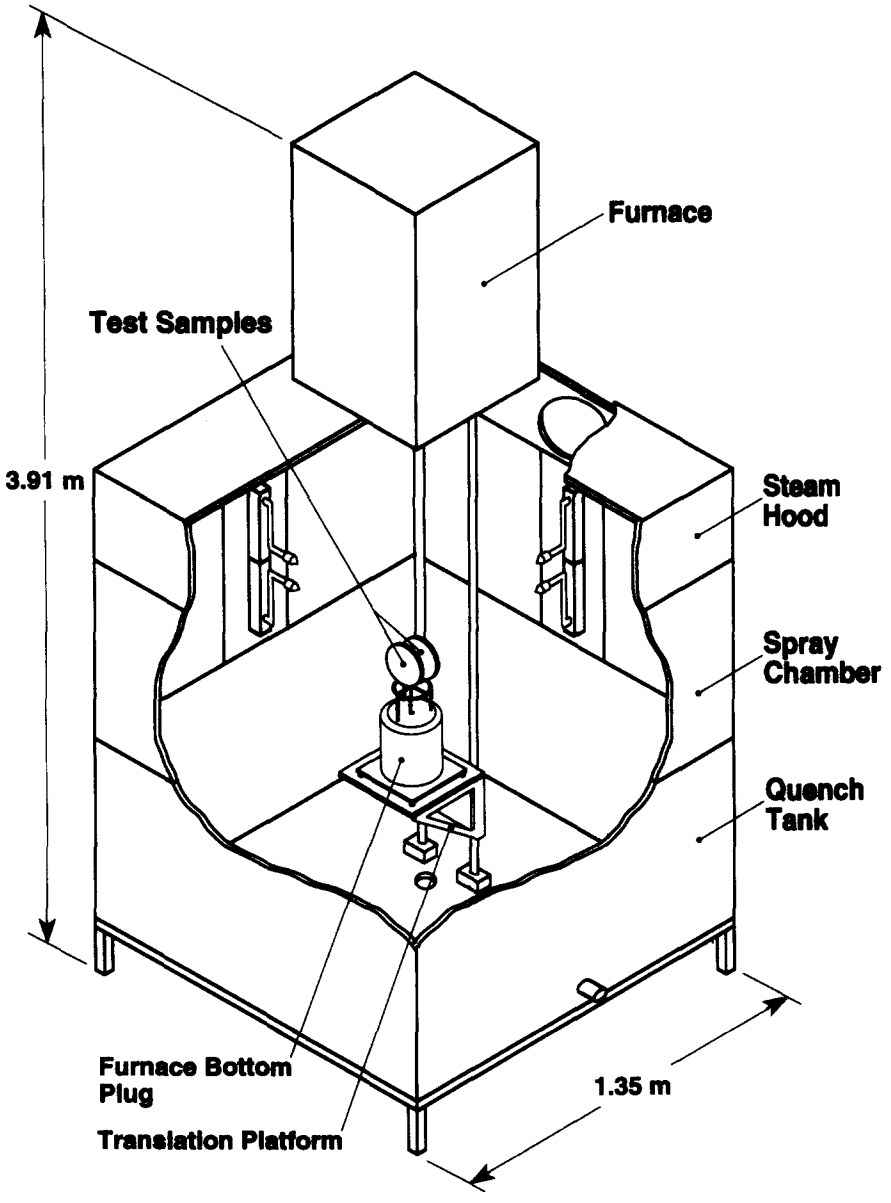

Fig. 3. Cut-away view of the materials processing test bed.

$$Sk = \frac{1}{\sigma^3}\int_{-\infty}^{+\infty}(z-\bar{z})^3 p(z)\,dz, \tag{4}$$

and in discrete form,

$$Sk = \frac{1}{\sigma^3 N}\sum_{i=1}^{N}(z_i-\bar{z})^3. \tag{5}$$

The surface height distribution for a surface which is flat except for a few bumps would possess a definite shift or positive skewness towards positive height values. Conversely, a negative skewness is indicative of a flat surface with a few pits.

Kurtosis is a measure of the peakedness of the surface height distribution and gives an indication of the degree of data spread. The normalized kurtosis is defined mathematically as the fourth moment of surface height about the mean minus 3.

$$Ku = \frac{1}{\sigma^4}\int_{-\infty}^{+\infty}(z-\bar{z})^4 p(z)\,dz - 3, \tag{6}$$

and in discrete form

$$Ku = \frac{1}{\sigma^4 N}\sum_{i=1}^{N}(z_i-\bar{z})^4 - 3. \tag{7}$$

A surface with a relative large number of bumps and pits (i.e. sharp surface height changes) will have a normalized kurtosis value greater than zero, whereas a relatively flat surface with a few bumps or pits will have a value less than zero. A surface with a normal

(Gaussian) distribution has a normalized kurtosis value of zero.

Dimensionless autocovariance function

The autocovariance function is the product of two 'copies' of the same surface profile as one profile is shifted relative to the other by some finite lag length l. A high positive value of the autocovariance function indicates the surface has a tendency to repeat itself for that particular lag length. Mathematically, the autocovariance function for a sample length L in a spatial direction x is defined as

$$C(l) = \lim_{L\to\infty} \frac{1}{L}\int_0^L \{z(x)-\bar{z}\}\{z(x+l)-\bar{z}\}\,\mathrm{d}x. \quad (8)$$

The finite sample approximation for equation (8) is

$$C(k) = \frac{1}{N}\sum_{i=1}^{N-k} \{z_i-\bar{z}\}\{z_{i+k}-\bar{z}\} \quad k = 0, 1, \ldots, N-1, \quad (9)$$

where k is the integer corresponding to the lag length, its value being the ratio of lag length, l, to the distance, l_0, between consecutive scan points (1 μm in the present measurements). In the present study, the autocovariance function was determined for portions of the scan length corresponding to k values up to 256 (i.e. 2^8).

The dimensionless autocovariance function, $A(k)$, is sometimes used instead of the autocovariance function. It is a dimensionless ratio with an absolute value less than or equal to unity, defined as the ratio of the autocovariance function for a given lag length to the same function for zero lag.

$$A(k) = \frac{C(k)}{C(0)}. \quad (10)$$

For a finite sample, equation (10) reduces to

$$A(k) = \frac{1}{\sigma^2 N}\sum_{i=1}^{N-k} \{z_i-\bar{z}\}\{z_{i+k}-\bar{z}\} \quad k = 0, 1, \ldots, N-1. \quad (11)$$

Periodogram

A Fourier analysis of a data series decomposes the finite series into a sum of sinusoidal components whose wavelengths are integral submultiples of the series period. A Fourier transform of the dimensionless autocovariance of surface roughness data (called the power spectral density) determines which frequencies are present in the Fourier series and, hence, in the surface profile data itself. This allows conversion of data from a space domain to a frequency domain.

A popular method for estimating the power spectral density function is the periodogram, which is represented mathematically as [7, 8]

$$I(\omega) = \frac{1}{2\pi N}\left|\sum_{i=1}^{N}(z_i-\bar{z})\mathrm{e}^{-i\omega i}\right|^2. \quad (12)$$

The dimensionless spatial frequency, ω, in equation (12) is related to spatial wavelength, λ_n, by

$$\omega_n = \frac{2\pi}{N}\frac{L}{\lambda_n} = \frac{2\pi n}{N} \quad n = 0, 1, \ldots, N/2. \quad (13)$$

The periodogram determines the relative importance of wavelengths (surface feature sizes) in the range of $2l_0 \leqslant \lambda_n \leqslant L$ in describing the surface profile.

4. RESULTS AND DISCUSSION

Data matrix

Experiments were first performed with Al-1100 samples in order to compare the roughening trends associated with a heat-spray quench cycle for polished, particle blasted and milled finishes. Comparing these trends to those resulting from air cooling facilitated a controlled study of possible roughening effects such as *surface chemical reactions*, *mineral deposition* (caused by evaporation of spray droplets) and *surface deformation* (caused by droplet impact). Experiments were then repeated with the popular alloy Al-2024 to determine whether *composition* or differences in *heat treatment temperature* have any significant effects on roughness.

While SEM and chemical analysis provide valuable accounts of surface structure and composition, these techniques do not give complete information on the changes in magnitude of surface roughness. Statistics, using profilometry data, can show which surface features are most dominant as well as whether features of a given size develop or diminish as a result of the heat–quench cycle.

A number of statistical parameters were employed in analyzing the roughness data taken with the profilometer. The average roughness, R_a, was the key parameter used in comparing roughness trends for the different surfaces and different heat treatment methods. The other statistical parameters were applied only for the primary data matrix of Al-1100 samples undergoing a heat-spray quench cycle. In using these parameters, it is important to recognize both the limitations and resolution of surface profilometry. As mentioned earlier, a diamond tip stylus with a 1.5 μm radius was used in the measurements. Resolution of surface cavities and other features captured by the profilometer is limited by the size of the stylus. Some of the cavities captured in SEM images were of the same size as the stylus tip, rendering inaccurate the characterization of these cavities, especially the cavity depth. Furthermore, any sharp subfeatures within relatively large cavities prevent the stylus from tracing the precise inner contour of these cavities. The accuracy of the profilometer data increases with increasing feature size. The features best characterized in the present measurements are those which are large

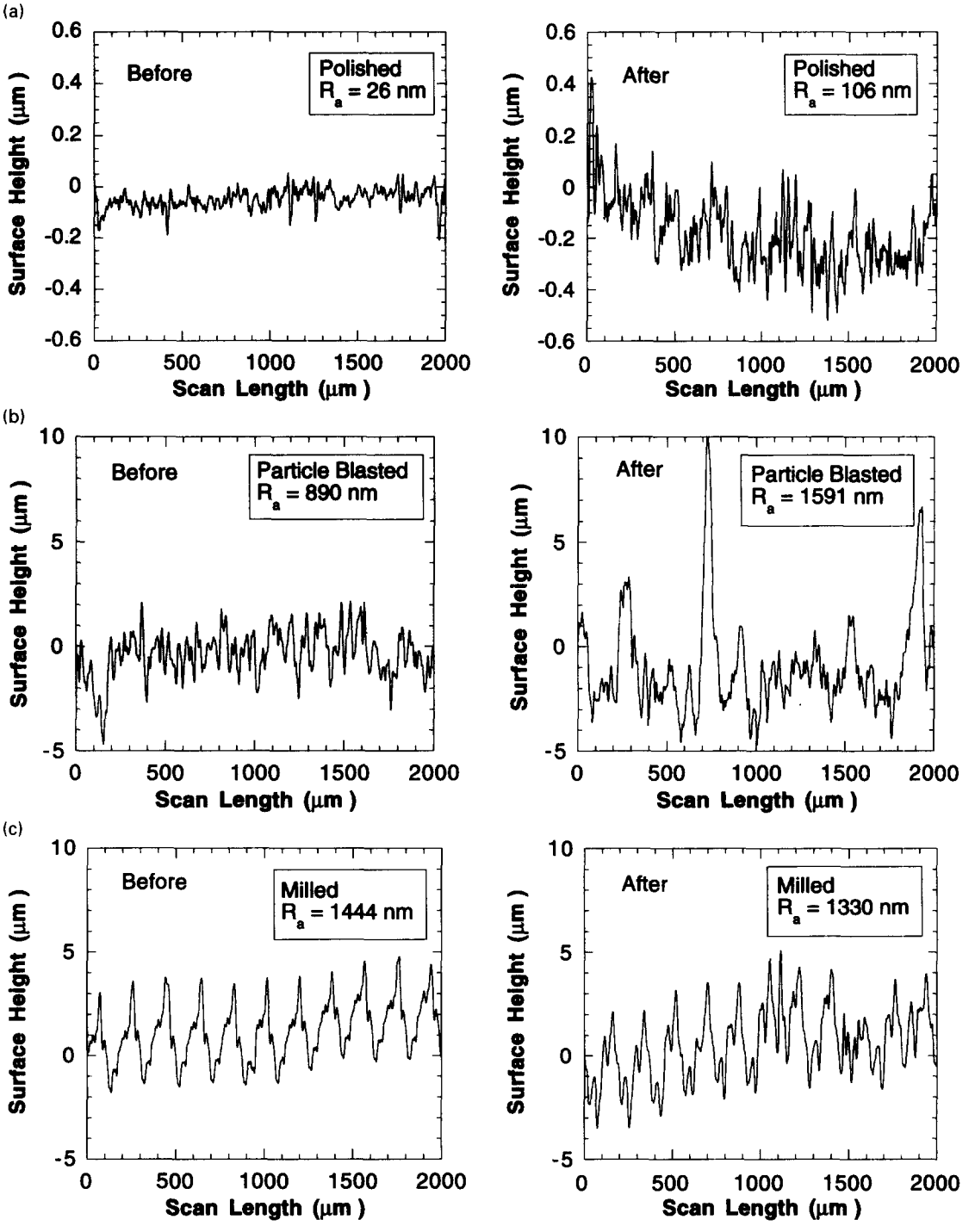

Fig. 4. Surface profiles for Al-1100 samples with (a) polished, (b) particle blasted, and (c) milled finishes before and after a heat-spray quench cycle.

enough to affect the droplet impact, spreading the breakup characteristics which are known to greatly influence the Leidenfrost temperature.

4.1. *Al-1100 heat-spray quench results*

Surface profiles. Figure 4a–c shows typical surface profiles measured by the profilometer for the polished, particle blasted, and milled surfaces before and after a heat-spray quench cycle. The ordinate on the polished surface plots, Fig. 4a, is magnified to better illustrate the surface features. The surface profiles show that the heat–quench cycle resulted in changes which are dependent upon the initial roughness. Average roughness on the polished surface and particle blasted sur-

face increased about four times and two times, respectively, while the milled surface showed only a small fractional change. The polished sample's profile, Fig. 4a, indicates roughening on a relatively small wavelength scale (up to 25 μm) evidenced by more pronounced surface features following, as compared to before, the heat–quench cycle. Large peaks with relatively large wavelengths, 100–200 μm, are visible in the particle blasted sample's post heat–quench profile, Fig. 4b. It is interesting to note the particle blasting process employed in the initial preparation of the surface produced features of about 5–10 μm, which are much smaller than those measured following the quench.

The post heat–quench profiles for both the polished and particle blasted surfaces are consistent with SEM images of the same surfaces. Both the microscopic changes which occurred on both the polished and particle blasted surfaces and the relatively large scale changes on the particle blasted surface were caused by a hydrogen diffusion phenomenon resulting from breakdown of water molecules during high temperature oxidation of aluminum and other metallic surfaces [3, 9–12]. While reacting with the aluminum surface to form an oxide, water vapor breaks down, forming atomic hydrogen which diffuses into the metal surface where it combines to form molecular hydrogen. This molecular hydrogen accumulates at sites of surface discontinuity such as voids and grain boundaries, producing regions of very high pressure. Since points of discontinuity on the polished sample are exposed to the surface, the hydrogen molecules can be released by breaking through the surface leaving small pits as shown in Fig. 5a. The particle blasted surface, on the other hand, is made up of an initial leafy structure which provides an abundance of relatively large accumulation sites for the hydrogen molecules over a wide range of surface depths. Instead of breaking through the surface, the molecular hydrogen formed deep into the metal produces relatively large bumps or blisters, some measuring as large as 1000 μm. Figure 5b clearly depicts a large distribution of such blisters. Continuing studies by the authors reveal a droplet with a diameter of 0.286 mm (Sauter mean diameter of the spray) will spread out into a 10–50 μm thick liquid film upon impact on a smooth surface. Therefore, large blisters will undoubtedly influence the impact and spreading of the spray droplets and, consequently, the Leidenfrost temperature, as was indeed demonstrated experimentally by Bernardin [4].

The periodic features in the profile of the milled surface, Fig. 4c, represent surface grooves left behind by the mill bit as it traversed the surface. The pre- and post-heat–quench profiles for this sample are very similar; the minor differences being due to the different locations for the profile measurements. The large surface features associated with the milling process seem to dwarf any oxidation or hydrogen diffusion effects of the heat–quench cycle.

Statistical results. Figure 6a–c show the surface height distributions for the polished, particle blasted and milled samples, respectively, before and after a heat–quench cycle. The polished sample's distribution for the pre-heat–quench case is fairly tight about the mean roughness. The high peak and lack of spread in the distribution are representative of a very flat surface evidenced by the small skewness for this distribution. The distribution for the post-heat–quench surface has a much wider spread, indicating a much rougher surface with many pits, such as those depicted in Fig. 5a. The depressions within these pits contribute to a broader negative surface height spread, while the rims of the same pits contribute to a broader positive height spread.

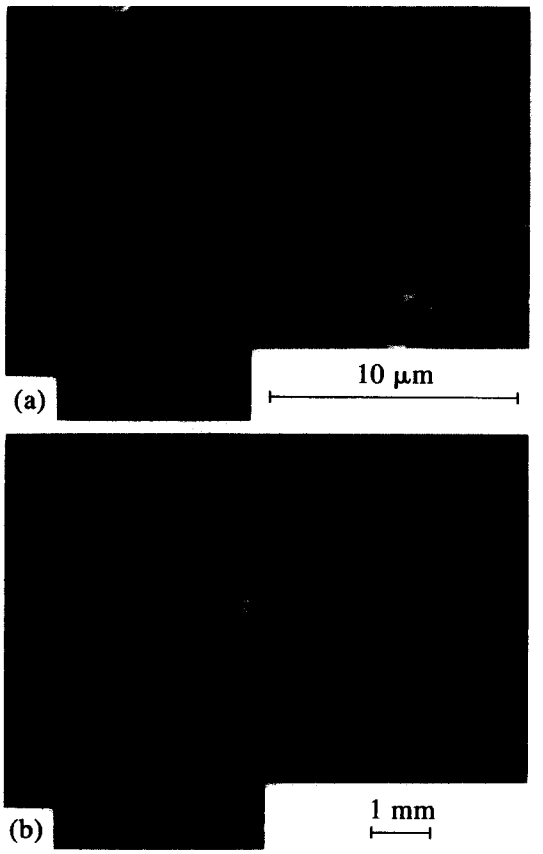

Fig. 5. (a) Pitting on an Al-1100 polished sample and (b) blistering on an Al-1100 particle blasted sample following a heat-spray quench cycle.

For the particle blasted sample, the pre-heat–quench distribution is symmetrical about the mean surface height with a near zero skewness and a normalized kurtosis value of -1.97, indicating a lack of extreme data spread. The surface height distribution for this sample following the heat–quench cycle is flatter and broader. The skewness and normalized kurtosis of the post heat treatment distribution are 1.98 and 2.30, respectively, which suggest the development of large surface bumps during the heat–quench process, Fig. 5b, which is in agreement with the surface profiles shown in Fig. 4b.

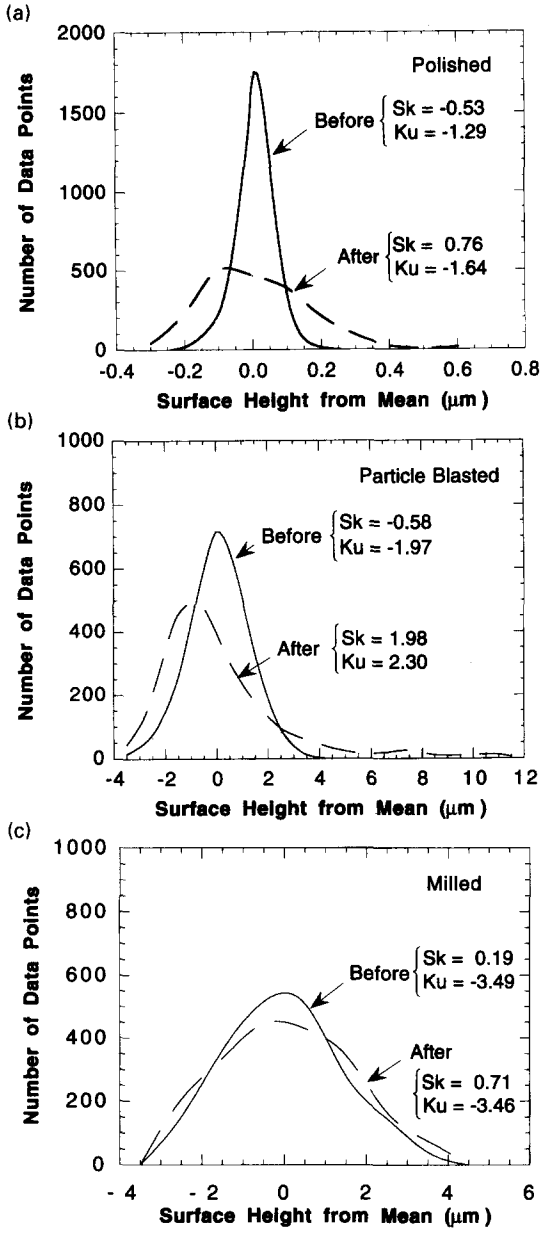

Fig. 6. Surface height distributions for Al-1100 samples with (a) polished, (b) particle blasted, and (c) milled finishes before and after a heat–spray quench cycle.

As shown in Fig. 6c, the surface height distribution for the milled surface did not change significantly following the heat–quench cycle. This is supported by the nearly identical skewness and kurtosis values for the pre- and post-heat–quench surface height distributions.

The surface profiles were also examined using the dimensionless autocovariance and periodogram. These statistical tools were used to distinguish any periodic surface features from the apparent randomness of the surface and determine the wavelengths (sizes) of the dominant features. The dimensionless autocovariance and periodogram for the polished, particle blasted, and milled samples are shown in Figs. 7 and 8, respectively. The two data sets of 256 scan points provided for each sample reveal general repeatability in surface features. The differences between results from each scan are typical of surface roughness measurements.

The dimensionless autocovariance functions for the polished sample before and after the heat–quench cycle are noticeably different as shown in Fig. 7a. Both reveal some periodicity in the surface features as indicated by the minimum and maximum points in the individual plots; the relative importance of the different feature sizes is highlighted in the corresponding periodograms. Figure 8a shows a few relatively large features developed after the quench; however, the small magnitude of the periodogram (the y-axis for the polished surface periodogram is magnified for clarity) and relatively poor repeatability following the heat–quench cycle indicate these features are by no means dominant in characterizing the polished surface following the quench.

The dimensionless autocovariance function for the particle blasted sample, Fig. 7b, also exhibits differences between the pre- and post-heat–quench conditions. These and the periodogram differences shown in Fig. 8b are primarily the result of the development of relatively large features following the quench. These features are both significant and consistent with the formation of the hydrogen diffusion blisters captured in SEM images of the same surface as discussed earlier.

As shown in Fig. 7c, the dimensionless autocovariance function for the milled surfaces did not exhibit significant differences between pre- and post-heat–quench conditions. This behavior is also seen in the corresponding periodogram, Fig. 8c, where the frequency dependence of the surface features appears unaltered following the heat–quench cycle. These findings are consistent with the previously discussed statistical results for the milled surface.

4.2. *Spray quenching vs air cooling results for Al-1100*

Table 1 compares values of the arithmetic average roughness, R_a, for a heat-spray quench cycle to a heat–air cooling cycle. Shown in this table are the mean values of R_a from 10 separate scans made on the particular sample, and the corresponding standard deviation of the 10 values for the pre- and post-simulated heat treatment cycle. Also included are the absolute and percent change in R_a.

The polished sample exhibited the greatest percent change in average roughness with several fold increases for both the spray quenched and air cooled conditions. The increase in R_a of slightly over 100 nm was about the same for both conditions, proving there is little difference in roughening between spray quenching and air cooling. This result dismisses both the mineral deposition caused by the boiling of spray droplets and the mechanical deformation caused by droplet impact as having any significant roughening effects for polished surfaces. Interestingly, spraying

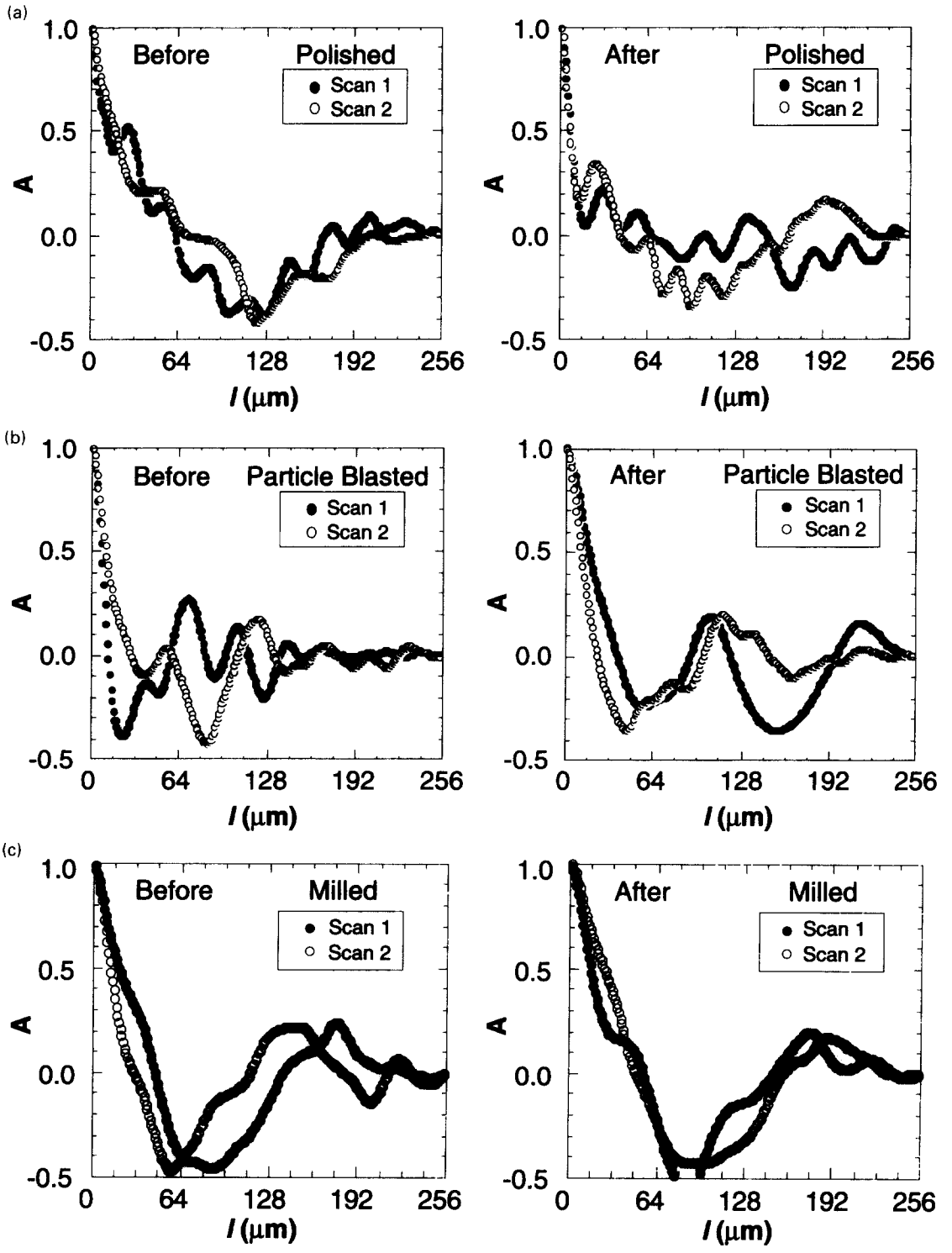

Fig. 7. Dimensionless autocovariance function of surface height for Al-1100 samples with (a) polished, (b) particle blasted, and (c) milled finishes before and after a heat–spray quench cycle.

the surface with water without preheating had a negligible effect on roughness (see Table 2), which supports the conclusions just made concerning the effects of both droplet impact and mineral deposition.

The particle blasted samples showed roughening trends similar to those of the polished samples. However, while the percent change in average roughness for these samples is much smaller than for the polished samples, the absolute change is nearly an order of magnitude greater, as shown in Table 1. As expected, the rougher surface showed a wider spread in the roughness data evidenced by the corresponding

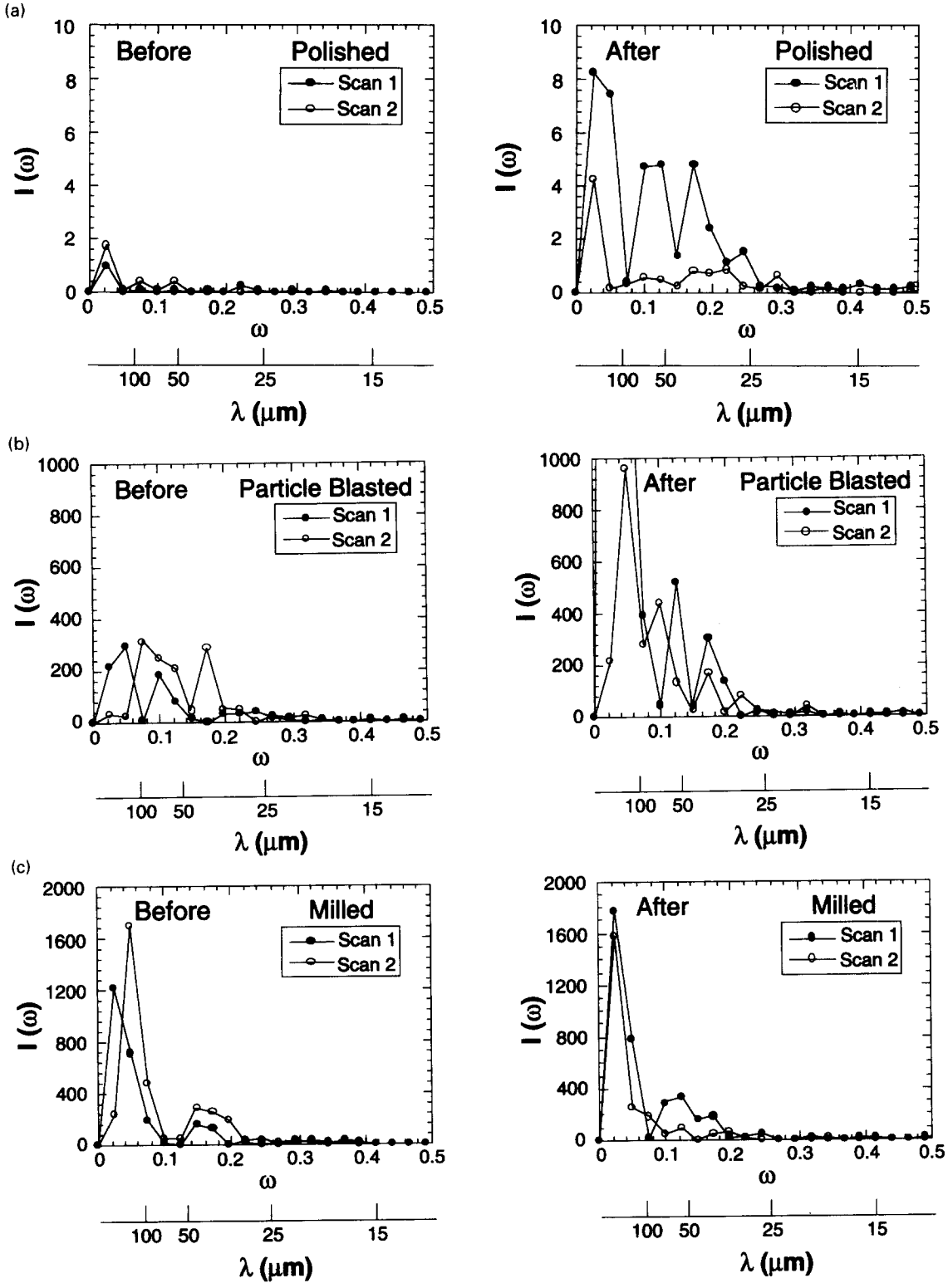

Fig. 8. Periodogram of surface height for Al-1100 samples with (a) polished, (b) particle blasted, and (c) milled finishes before and after a heat spray–quench cycle.

greater standard deviation of R_a values. These results illustrate that the changes in surface roughness are directly dependent upon the sample's surface condition before heating, as described earlier, in conjunction with the hydrogen diffusion blisters on the particle blasted samples. The relatively small differences in the magnitude of R_a between the spray quenched and air cooled samples are additional proof

Table 1. Comparison of Al-1100 average roughness results for heat-spray quenching and heat-air cooling cycles

Initial surface finish	Cooling process	R_a (nm) and standard deviation (nm) of 10 R_a values				ΔR_a (nm)	% R_a
		Before		After			
Polished	spray quenched	26	6	106	36	80	308
	air cooled	36	5	119	14	83	231
Particle blasted	spray quenched	890	207	1591	271	701	79
	air cooled	855	71	1506	371	651	76
Milled	spray quenched	1444	525	1330	683	114	7.9
	air cooled	1060	491	961	457	99	9.3

Table 2. Average roughness results for the Al-1100 secondary data matrix

Initial surface finish	Cooling process	Note	R_a (nm) and standard deviation (nm) of 10 R_a values				ΔR_a (nm)	% R_a
			Before		After			
Polished	spray quenched	heat–quench cycle repeated 3 times	33	16	185	42	152	461
	spray quenched	furnace plug sealed	17	5	40	12	23	135
	air cooled	furnace plug sealed	43	8	84	22	41	95
	none	no heatup, surface water sprayed	55	28	63	38	8	15
	spray quenched	heated to 495 instead of 555 °C	63	38	97	52	34	54
Particle blasted	3 spray quenches	heat–quench cycle repeated 3 times	915	91	2421	455	1506	165
	spray quenched	furnace plug sealed	845	98	874	80	29	3
	air cooled	furnace plug sealed	899	119	1016	143	117	13

that mineral deposition and droplet impact do not play a significant role in the roughening of aluminum surfaces.

Table 1 shows that the changes in R_a for the milled samples, both on an absolute or percent basis, are much smaller than those of the particle blasted samples. Additionally, both spray quenching and air cooling seem to produce about the same roughness changes. One noteworthy trend with the milled surface results is the relatively large standard deviations of the R_a values. These large standard deviations resulted from the unique nature of the milled surface. While this surface may seem fairly uniform, it contains features of a much larger scale than found on the particle blasted or polished samples. These features are also direction dependent and influenced by such factors as cutter speed, feed rate, cutter sharpness, cut depth and lubrication. Thus, the measured features of a milled surface can vary from sample to sample and even with scan direction on the same sample, resulting

in a surface that is difficult to characterize with certainty.

The R_a trends indicated in Table 1 are very instrumental at discounting both mineral deposition and mechanical deformation as important causes for the roughness changes. These trends also emphasize the role of hydrogen diffusion in the roughening, but fail to explain why this phenomenon would produce equal roughness changes in both spray quenching and air cooling. This important issue will be discussed in the next section.

Al-1100 *secondary data matrix.* The secondary data matrix, described in Table 2, was established to account for or to separate out factors responsible for the surface roughening of the Al-1100 samples which could not be identified clearly with the Al-1100 matrix described in Table 2. In the secondary matrix, only the polished and particle blasted surfaces were examined, since the milled surface showed relative insensitivity to roughening effects as demonstrated by the statistical results presented earlier.

To account for the additive oxidation and associated hydrogen diffusion effects, polished and particle blasted samples of Al-1100 were run through three consecutive heat-spray quench cycles. The polished sample experienced a 461% increase in R_a, whereas the particle blasted sample's roughness increased by 165%. These values are higher than the corresponding values of 308 and 74% measured on the polished and particle blasted samples, respectively, following a single heat-spray quench cycle. These results suggest repeated heat–quench cycling increases the surface roughness, which increases the Leidenfrost temperature and accelerates the cooling process as shown in Fig. 1b.

To further investigate the hydrogen diffusion effects, a few tests were performed in which the porous plug which insulated the furnace underside during the preheating was carefully sealed to prevent steam from entering the furnace. Comparing the results from Tables 1 and 2 shows a significant decrease in R_a for the polished samples, from 308 to 135% for spray quenching, and from 231 to 95% for air cooling. The decrease in R_a for the particle blasted samples was even more drastic, from 79 to only 3% for spray quenching, and from 76 to 13% for air cooling. Interestingly, surface blistering was not observed on the particle blasted samples when the furnace plug was sealed.

These results suggest that (1) hydrogen diffusion is a major contributor to the increase in surface roughness; (2) this phenomenon results from exposure of the surface to steam at very high temperatures during heat-up inside the furnace, and not the subsequent spray quenching or air cooling; and (3) the pitting and blistering induced by hydrogen diffusion can be controlled by reducing the amount of steam present in the heat treating furnace. However, total elimination of steam may not be practical in industrial heat treating since aluminum parts are often solution heat treated in moisture laden furnaces.

4.3. *Al*-2024 *results*

The presence of alloying elements (mainly copper) in Al-2024 reduces the melting point for this alloy relative to Al-1100. In fact, the recommended solution heat treatment temperature for Al-2024 is 495°C [13], 60°C lower than the heat-up temperature for Al-1100 samples. Therefore, in order to compare the roughening effects for the two materials corresponding to equal preheating temperatures, a polished Al-1100 sample was put through a temperature history identical to that of Al-2024. Figure 9a displays the surface pitting found earlier on an Al-1100 sample after heating to 555°C. As shown, respectively, in Figs. 9b and 9c, pitting was present to a lesser degree on a polished Al-1100 sample and was nonexistent on a polished sample of Al-2024, both heated to 495°C and spray quenched. Instead of pitting, small white patches of the order of a few microns are visible across the Al-2024 surface. A dispersive X-ray scan revealed these patches were copper-rich grains composed of 77% aluminum and 23% copper by weight. Comparing the results from Tables 1 and 3 shows that the Al-2024 sample exhibited a 27% increase in R_a, compared to 54% for the Al-1100 sample.

Table 3 gives a summary of roughening trends for Al-2024 samples with polished, particle blasted, and extruded surfaces, which were preheated to 495°C. Most noticeable when comparing these results to those of Al-1100 samples which were preheated to 555°C (Table 1), are the negligible changes in roughness associated with the heat-spray quench cycle for Al-2024. The polished and particle blasted Al-2024 samples exhibited 27 and 2% increases in R_a, respectively, compared to 308 and 79% for the Al-1100 samples. An extruded Al-2024 sample experienced a 13% increase in roughness, which was confirmed by a lack of any significant differences in SEM images of the surface taken before and after a heat-spray quench cycle.

These findings clearly demonstrate Al-2024 undergoes markedly smaller changes in roughness than Al-1100 because of the presence of the alloying elements in Al-2024, and, more importantly, because the lower furnace temperature for Al-2024 reduces the oxidation and associated hydrogen diffusion effects.

5. CONCLUSIONS

Experiments were performed and statistical methods employed to explore all the possible causes for surface roughening of aluminum during heat treatment. Samples with different initial finishes were subjected to a variety of simulated heat treatment techniques and examined using both SEM and surface contact profilometry prior to and after heat treatment. Key conclusions from the study are as follows:

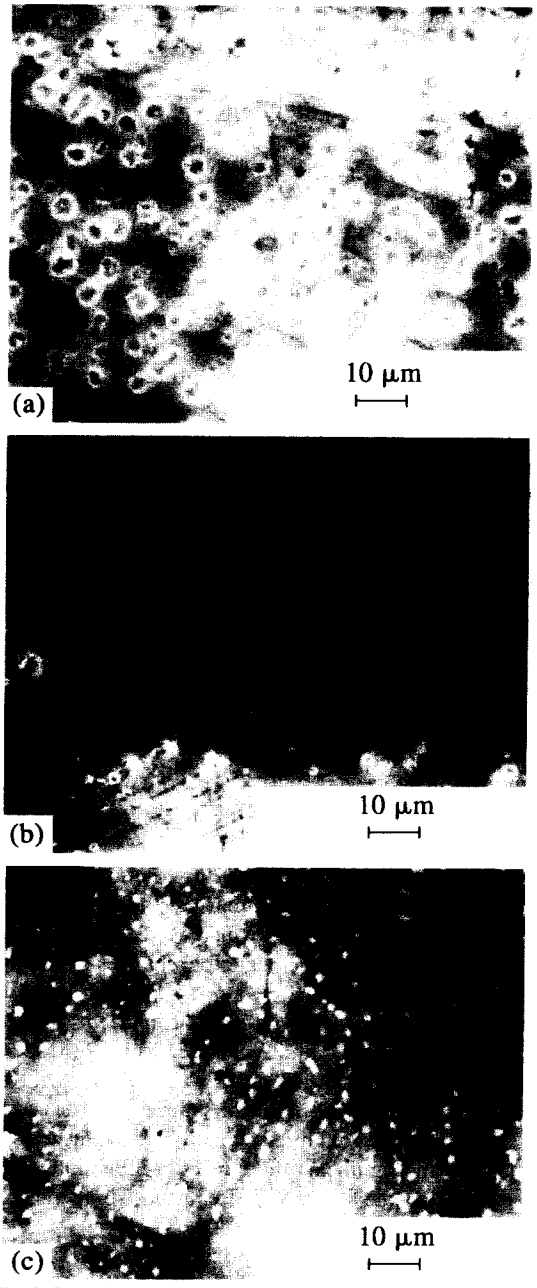

Fig. 9. Scanning electron microscope images taken following a heat–spray quench cycle for (a) polished Al-1100 surface preheated to 555°C, (b) polished Al-1100 surface preheated to 495°C, and (c) polished Al-2024 sample preheated to 495°C.

(1) Al-1100 samples with different initial finishes experienced different changes in roughness. Polished and particle blasted surfaces showed an increase in roughness following a heat-spray quench cycle. This trend was not observed with milled surfaces.

(2) Mineral deposition associated with droplet evaporation and the dynamic forces associated with droplet impact had no measurable effects on surface roughness.

(3) Most of the roughening was the result of a hydrogen diffusion phenomenon resulting from the breakdown of water molecules during high temperature oxidation of the aluminum surface. This phenomenon resulted in the creation of surface pits and blisters on the polished and particle blasted surfaces, respectively, Al-1100 samples. A necessary condition for the occurrence of the hydrogen diffusion phenomenon is the existence of moisture in the heat treating furnace. In fact, most of the pitting and blistering occurred due to the breakdown on water vapor at high temperatures within the furnace, and not due to the spray quenching. Lowering the furnace temperature from 555 to 495°C eliminated much of the pitting and blistering on the Al-1100 samples.

(4) Surface roughness features, which develop during a heat–quench cycle, can influence the cooling characteristics of the surface to various degrees. Pitting and other small scale roughness features up to about 25 μm increase the bubble nucleation density during the transition and nucleate boiling regimes, while blisters and other large roughness features on the order of a droplet size (25 to 1000 μm) influence the impact and spreading of the spray droplets and, consequently, the Leidenfrost temperature.

(5) Al-2024 samples with polished, particle blasted, and extruded surface finishes did not experience significant increases in surface roughness during heat treatment because of both its alloying elements and its relatively low solution heat treatment temperature.

Acknowledgement—Financial support for this work by the National Science Foundation, through the Purdue University Engineering Research Center for Intelligent Manufacturing Systems, is gratefully appreciated.

REFERENCES

1. J. R. Thome, *Enhanced Boiling Heat Transfer*. Hemisphere, New York (1990).

Table 3. Average roughness results for Al-2024 samples prior to and following a heat-spray quench cycle

Initial surface finish	Cooling process	R_a (nm) and standard deviation (nm) of 10 R_a values					
		Before		After		(nm)	% R_a
Polished	spray quenched	55	36	70	49	15	278
Particle blasted	spray quenched	886	244	866	332	−20	2
Extruded	spray quenched	1137	360	1288	502	151	13

2. J. C. Rozzi, W. P. Klinzing and I. Mudawar, Effects of spray configuration on the uniformity of cooling rate and hardness in the quenching of aluminum parts with nonuniform shapes, *J. Mater. Engng Performance* **1**, 49–60 (1992).
3. J. D. Bernardin and I. Mudawar, An experimental investigation into the relationship between temperature-time history and surface roughness in the spray quenching of aluminum parts, *ASME J. Mater. Technol.* (in press).
4. J. D. Bernardin, Intelligent heat treatment of aluminum alloys: material, surface roughness, and droplet-surface interaction characteristics, Masters Thesis, School of Mechanical Engineering, Purdue University, West Lafayette, IN (1993).
5. H. C. Ward, Profile description. In *Rough Surfaces* (Edited by T. R. Thomas), pp. 72–90. Longman, New York (1982).
6. R. D. Gibson, The surface as a random process. In *Rough Surfaces* (Edited by T. R. Thomas), pp. 119–143. Longman, New York (1982).
7. W. A. Fuller, *Introduction to Statistical Time Series*, p. 275. Wiley, New York (1976).
8. M. B. Priestley, *Spectral Analysis and Time Series*. Academic Press, New York (1981).
9. U. R. Evans, *The Corrosion and Oxidation of Metals: Scientific Principles and Practical Applications*. Arnold, London (1960).
10. J. D. Fast, *Interactions of Metals and Gases*. Academic Press, New York (1965).
11. H. Y. Hunsicker, The metallurgy of heat treatment. In *Aluminum: Properties, Physical Metallurgy and Phase Diagrams*, Vol. 1, pp. 109–162. ASM, Metals Park, OH (1967).
12. U. R. Evans, *The Corrosion of Metals: First Supplementary Volume*. St Martin's Press, New York (1968).
13. *ASM Handbook*, Vol. 4 (10th Edn). ASM International, Materials Park, OH (1991).